Exposure of Cultured Hippocampal Neurons to the Mitochondrial Uncoupler CCCP Induces a Rapid Growth of Dendritic Processes

Lilia Kushnireva , Eduard Korkotian , Menahem Segal *

Posted Date: 4 August 2023

doi: 10.20944/preprints202308.0380.v1

Keywords: CCCP, Carbonyl Cyanide m Chlorophenyl Hydrazone; calcium; Orai1; STIM1; mitochondria

Article

Exposure of Cultured Hippocampal Neurons to the Mitochondrial Uncoupler CCCP Induces a Rapid Growth of Dendritic Processes

Liliia Kushnireva [1,2], Eduard Korkotian [2] and Menahem Segal [2,*]

[1] Faculty of Biology, Perm State University, Perm, Russia.; lilikushnireva@gmail.com
[2] Department of Neurobiology, Weizmann Institute of Science, Rehovot, Israel; eduard.korkotian@weizmann.ac.il
* Correspondence: menahem.segal@weizmann.ac.il; Tel.: 972 89342553

Abstract: A major route for influx of calcium ions into neurons uses the STIM-Orai1 voltage-independent channel. Once cytosolic calcium ($[Ca^{2+}]i$) elevates, it activates mitochondrial and endoplasmic calcium stores, to affect downstream molecular pathways. In the present study we employed a novel drug, Carbonyl Cyanide Chlorophenylhydrazone (CCCP), a mitochondrial uncoupler, to explore the role of mitochondria in cultured neuronal morphology. CCCP caused a sustained elevation of $[Ca^{2+}]i$ and, quite surprisingly, a massive increase in density of dendritic filopodia and spines in the affected neurons. This morphological change can be prevented in cultures exposed to calcium-free medium, to Orai1 antagonist 2APB, or to cells transfected with dominant-negative Orai1 plasmid. It is suggested that CCCP activates mitochondria through influx of calcium, to cause a rapid growth of dendritic processes.

Keywords: CCCP; carbonyl cyanide m chlorophenyl hydrazone; calcium; orai1; STIM1; processes; mitochondria

1. Introduction

Variations in cytosolic calcium concentrations ($[Ca^{2+}]i$) play a crucial role in neuronal growth, communication, plasticity and survival. $[Ca^{2+}]i$ is accumulated in calcium stores, including endoplasmic reticulum and mitochondria so as to maintain a very low ambient $[Ca^{2+}]i$ (4-5 orders of magnitude below extracellular $[Ca^{2+}]$). This is controlled by voltage and ligand-gated calcium entry and by extrusion channels. Recent evidence assigned a pivotal role of stromal interaction molecule 1 (STIM1) in regulation of $[Ca^{2+}]i$ [1]. Accordingly, STIM-1 clusters near the depleted store, relocates to the membrane, where it activates Orai1 plasma membrane voltage-independent calcium channel to allow calcium influx into the cell, to refill the stores [2]. The interaction of stores/STIM/Orai has been studied extensively in non-neuronal cells [3]. Relatively less is known about their role in central neurons. STIM1 and Orai1 are localized in the brain [4], and can be converted from a dispersed to a punctate form upon depletion of calcium stores with thapsigargin [5]. They are important in regulation of growth cone motility [6,7], in regulation of voltage-gated calcium channels [8] and in detrimental effects of chronic epilepsy [9], ischemia [10] and oxidative stress [11]. While STIM1 has been imaged in punctate form in dendrites of hippocampal neurons [12], the dynamic distribution and function of Orai1 in such neurons remained enigmatic [13]. In the present study, we combined time-lapse imaging with pharmacological tools to explore the role of Orai1 in cultured hippocampal neurons. We used a mitochondria uncoupler Carbonyl Cyanide Chlorophenylhydrazone (CCCP), which increases proton permeability and depolarizes mitochondrial membrane potential. Previously, we found that CCCP causes an increase in the frequency of spontaneous global calcium bursts with their subsequent complete disappearance [14]. We now demonstrate that longer exposure to CCCP induces $[Ca^{2+}]i$ rise in an Orai1 dependent manner, conjugate mitochondrial calcium saturation and massive growth of dendritic processes, followed by apoptotic swelling and subsequent death of the cultured hippocampal neurons.

Preprints (www.preprints.org) | NOT PEER-REVIEWED | Posted: 4 August 2023 doi:10.20944/preprints202308.0380.v1

2. Results

In the first series of experiments, we explored long term effects of CCCP on [Ca^{2+}]i and the formation of novel dendritic filopodia/spines. As can be seen in Figure 1, [Ca^{2+}]i, measured with the membrane permeant Fluo-2 AM, grows gradually over 30 minutes of exposure (Figure 1, A-C). In the same group of neurons, a significant increase in density of dendritic processes is clear at 30 minutes of exposure to the drug (Figure 1, A, D). To obtain a direct indication for the role of extracellular calcium ([Ca^{2+}]o) to change in [Ca^{2+}]i, the cells were maintained in nominally 0 mM calcium in the imaging medium. In these conditions, there was no change in [Ca^{2+}]i, and no change in filopodia/spines density (Figure 1, E-G). Upon replenishment of 2mM calcium in the medium, there was a rapid increase in [Ca^{2+}]i and a correlative increase in filopodia/spines density (Figure 1, E-G).

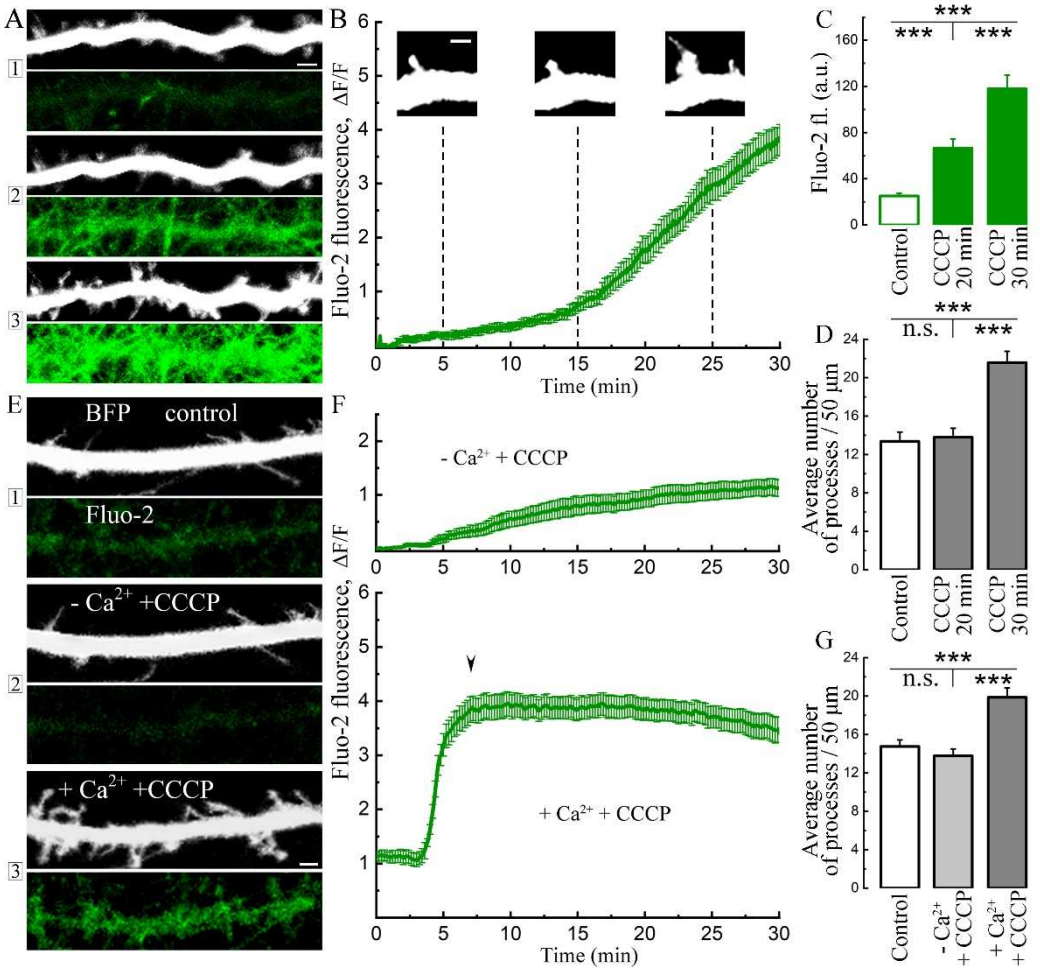

Figure 1. Effect of carbonyl cyanide 3-chlorophenylhydrazone (CCCP) on cytosolic calcium and growth of dendritic processes in hippocampal neurons. A. Dendritic segment from a neuron transfected with eBFP as a morphological marker (up, monochrome) and with Fluo-2 (bottom, green), cytosolic calcium sensor (1 - control, 2 - 20 min and 3 - 30 min with CCCP 10 µM). Scale 2 µm. **B.** The panel shows the mean (green trace) from 15 cell (bars indicate SEM). The calcium rise starts after 10-15 minutes of incubation with CCCP, at the beginning of which rare spontaneous calcium activity may still be observed. By 25 minutes the beginnings of new processes appear which show a sharp growth during the next 5 minutes of incubation. Scale 1 µm. **C.** Averaged Fluo-2 fluorescence in control conditions, 20 min and 30 min after treatment with CCCP. Control (normal medium): 25.13 ± 2.18, 20 min CCCP: 66.46 ± 8.04, 30 min CCCP: 117.85 ± 11.77 a.u.; F = 32.13; *** - $p < 0.001$, ANOVA, Bonferroni Post-hoc, n = 15 neurons (somata). **D.** Averages of dendritic processes detected with eBFP: control: 13.37 ± 0.96, 20 min CCCP: 13.8 ± 0.94, 30 min CCCP: 21.57 ± 1.19; F = 19.92; *** - $p < 0.001$, ANOVA, Bonferroni Post-hoc, n = 15 neurons, a comparable number of dendritic sections, 50 µm long,

 doi:10.20944/preprints202308.0380.v1

were analyzed for each cell. For **B-D**, cells from four cell cultures DIV 10-14 were used. **E.** Low calcium in the imaging solution (2), no effect of CCCP on cytosolic calcium and processes growth was observed (markers as in A). When calcium returned to the imaging medium, growth of processes was detected (3). Scale 2 μm. **F.** Only a slight increase in Fluo-2 fluorescence in low-calcium imaging medium was observed over a similar time course of the experiment as in B (green curve up). When calcium returned (2 mM) to the imaging medium (same experiment), after 3-5 min, a sharp abnormal increase of cytosolic calcium level was observed (bottom, green curve). The beginning time of spine / filopodia growth marked with arrowhead. **G.** Quantification of dendritic processes detected per 50 μm dendrite length using eBFP signal in normal medium compared to low calcium medium and same medium, when calcium was added: control: 14.75 ± 0.68, - Ca^{2+} + CCCP: 13.78 ± 0.71, Ca^{2+} back + CCCP: 19.88 ± 0.98; n.s. - not significant, F = 16.72; *** - $p < 0.001$, ANOVA, Bonferroni Post-hoc, n = 20 neurons from three cell cultures DIV 10-14.

There are several possible routes for entry of calcium into the neurons, that may facilitate formation of dendritic filopodia. To identify the route of calcium entry under the CCCP conditions, we exposed the cultures to different calcium antagonists, including APV, TTX and DNQX, nifedipine and conotoxin, as well as 2-APB, an antagonist of the Orai1-2 channels. The CCCP-induced increase in $[Ca^{2+}]i$ and growth of dendritic processes was completely blocked (average 17.26 ± 1.43 processes in control conditions and 17.65 ± 1.48 after 40 min with CCCP + 2-APB per 50 μm dendritic segments, not significant, t-test, n = 23 cells) by the use of 2-APB (Figure 2, A-B). Furthermore, cells transfected with the mutant Orai1(mOrai1) were resistant to the CCCP-induced rise in $[Ca^{2+}]i$ (Figure 2, E-G). In the presence of mOrai1, CCCP lead to only a slight increase in cytosolic calcium (Figure 2, G), and did not lead to a significant increase in processes (Figure 2 E, F). This indicates that CCCP is using the Orai channel to load the cell with $[Ca^{2+}]$. It should be noted that although other antagonists did not affect the overall increase in cytosolic calcium and the growth of new processes, some of them had their own isolated effects. Thus, the application of ω-conotoxin and nifedipine led to a short-term burst of network activity, probably due to inhibition of GABAergic neurons [15]. This led to a temporary increase in $[Ca^{2+}]i$ and a subsequent return to the baseline. In contrast, the use of thapsigargin caused a rapid but sustained increase in intracellular Ca^{2+}, which was not limited to the drug preincubation period. As a result, the action of CCCP began not from the basal, but from an already elevated $[Ca^{2+}]i$, which created the illusion of a suppression sign of the effect by thapsigargin (Figure 2, C). In fact, the total growth of $[Ca^{2+}]i$ in thapsigargin + CCCP was the same as in CCCP alone, and the outgrowth of protrusions was not reduced to a statistically significant extent.

Preprints (www.preprints.org) | NOT PEER-REVIEWED | Posted: 4 August 2023 doi:10.20944/preprints202308.0380.v1

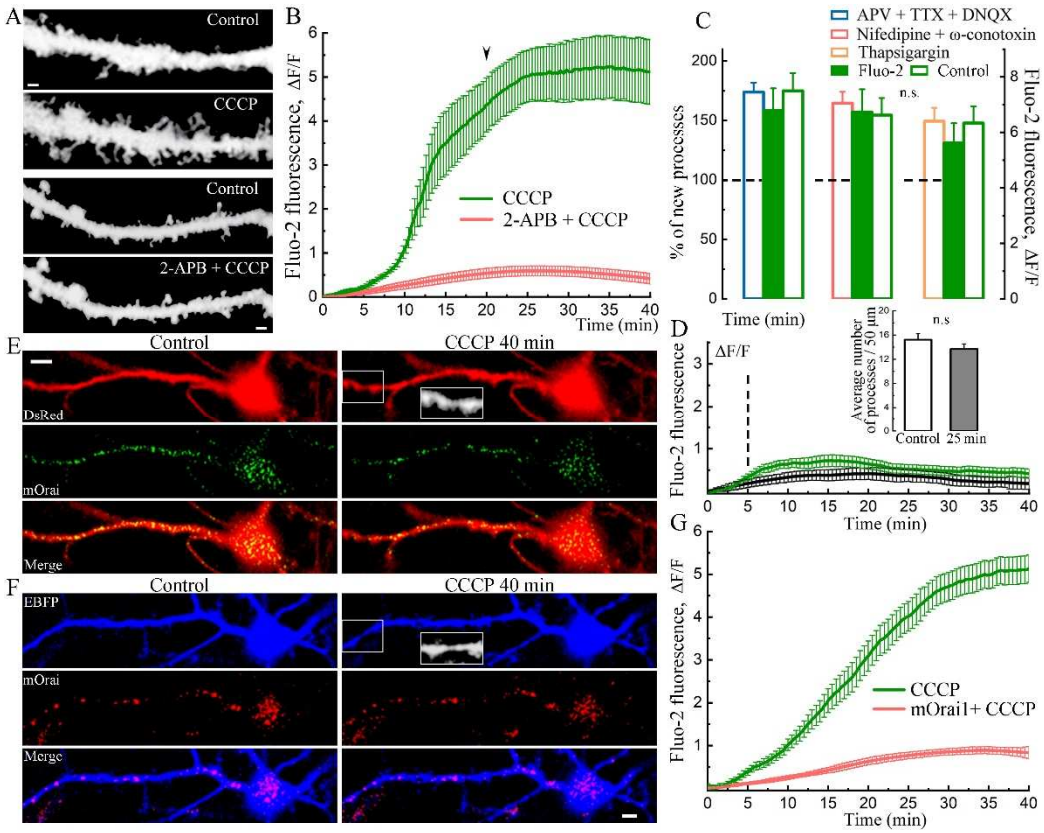

Figure 2. Effect of CCCP through the rise of [Ca²⁺]i on the growth of dendritic processes is depends on Orai. A. Growth of processes before and after 30 minutes of incubation with CCCP (eBFP, top two panels) in the presence of 2-APB 50 μM (two lower panels). Scale 2 μm. **B.** The effect of 2-APB 50 μM (n = 16 cells, carrot curve) on [Ca²⁺]i following CCCP. Control transfected cells (eBFP) with CCCP only: n = 15 cells, green curve, start of processes growth marked with arrowhead; three cell cultures, DIV 10-14. **C.** CCCP – induced rise of cytosolic calcium and dendritic processes is not inhibited by coincubation with the following blockers: thapsigargin 1 μM, nifedipine 1 μM + ω-conotoxin 50 nM, APV 30 μM + TTX 5 μM + DNQX 10 μM. Left bars of each set are measured in percent of existing/new processes, divided by dotted line. The percentage increases after 40 minutes of incubation with CCCP with the background of an increase in cytosolic calcium in transfected cells (green bars in group sets, n = 18 cells for each) and non-transfected cells (green right bars, n = 18 cells for each group). ANOVA, Fisher Post Hoc, three cell cultures. **D.** Cells were exposed to CCCP for 5 minutes and then (vertical mark) washed out (16 control transfected cells, green curve; 24 control non-transfected cells, black curve). After washing, [Ca²⁺]i approached basal levels and there was no process growth. Bars for control transfected (eBFP) cells, n = 16 cells, three cell cultures DIV 11-15. **E.** Cell transfected with mutant Orai1 (mOrai1) (green) did not grow dendritic processes in response to CCCP, but showed apoptotic swelling after 40 minutes of treatment (zoomed in white rectangle). Scale 5 μm. **F.** Cell transfected with red mOrai1 did not grow spines or filopodia, but showed apoptotic swelling after 40 minutes of CCCP treatment (zoom in white rectangle). Scale 5 μm. **G.** [Ca²⁺]i after CCCP treatment of cells transfected with mOrai1 (red curve, n = 16 cells) and control non-transfected cells in sight (green curve, n = 36 cells), three cell cultures DIV 10-14.

As a result of a small increase in cytosolic calcium that occurs in the experiment with mOrai1 (Figure 2, G), there was a slight tendency for the growth of new processes, however, this increase was not sufficient for a significant difference; mOrai1 / mOrai1 + CCCP 30 min: 15.87 ± 0.80 / 16.22 ± 0.86 processes, n = 16 cells, t-test. Since after a strong increase of cytosolic calcium level, the number of processes significantly increased, as showed in Figure 1, A, D and Figure 1 F (bottom) and G, it can be concluded that dendritic processes grow due to a sufficient increase in cytosolic calcium levels following CCCP-treatment. Interestingly, this effect does not appear when CCCP was extensively washed out after 5 minutes of incubation (Figure 2, D): control / CCCP wash: 15.23 ± 1.01 / 13.69 ±

 doi:10.20944/preprints202308.0380.v1

0.84, not significant, n = 16 cells, t-test. By itself, early washout did not prevent further neurotoxicity. New protrusion outgrowth and finally the appearance of dendritic blubs, the first signs of neurotoxicity and cell death, are shown on supplementary video S1. Thus, the appearance of new processes under the influence of CCCP is not directly related to its toxic effect on cells.

To further explore CCCP effects through the STIM-Orai pathway, we transfected neurons with normal Orai1, and in these neurons the presence of CCCP also lead the growth of new processes (Figure 3, A, B), similar to previous experiment in control conditions (Figure 1, D). We also shown that the process growth with CCCP does not depend on the characteristics of eBFP as a morphological marker, since an experiment was carried out with another morphological marker, DsRed (Figure 3, A). This indicates that the transfection itself is not responsible for the increase in $[Ca^{2+}]i$ or the density of newly-formed protrusions. We also observed an insignificant decrease in the fluorescence of normal Orai in neuronal somata, in contrast to its increase in distal dendrites, upon exposure to CCCP (Figure 3, C), possibly demonstrating the mechanism of Orai1 redistribution caused by SOCE activation [16]. It should also be noted that newly formed filopodia/spines were dynamically visited by Orai1 puncta, in agreement with our earlier observations [17]. On average, the size of STIM1 puncta decreased under CCCP (Figure 3, D-F).

To rule out a possible impact of overexpressed phenotype of the constructs used in the study (morphological markers and versions of Orai1), we compared the level of $[Ca^{2+}]i$ in non-transfected cells exposed to CCCP with transfected ones (Supplementary Figure 1, A). Without CCCP, transfected cells were spontaneously active and did not reveal a tendency to increase $[Ca^{2+}]i$ level during the entire period of recording (Supplementary Figure 1, ibid). Following CCCP, $[Ca^{2+}]i$ levels increased to the same extent and with about the same kinetics as non-transfected neurons (Supplementary Figure 1, A&B). Therefore, we conclude that transfection by itself has no effect on $[Ca^{2+}]i$.

Preprints (www.preprints.org) | NOT PEER-REVIEWED | Posted: 4 August 2023 doi:10.20944/preprints202308.0380.v1

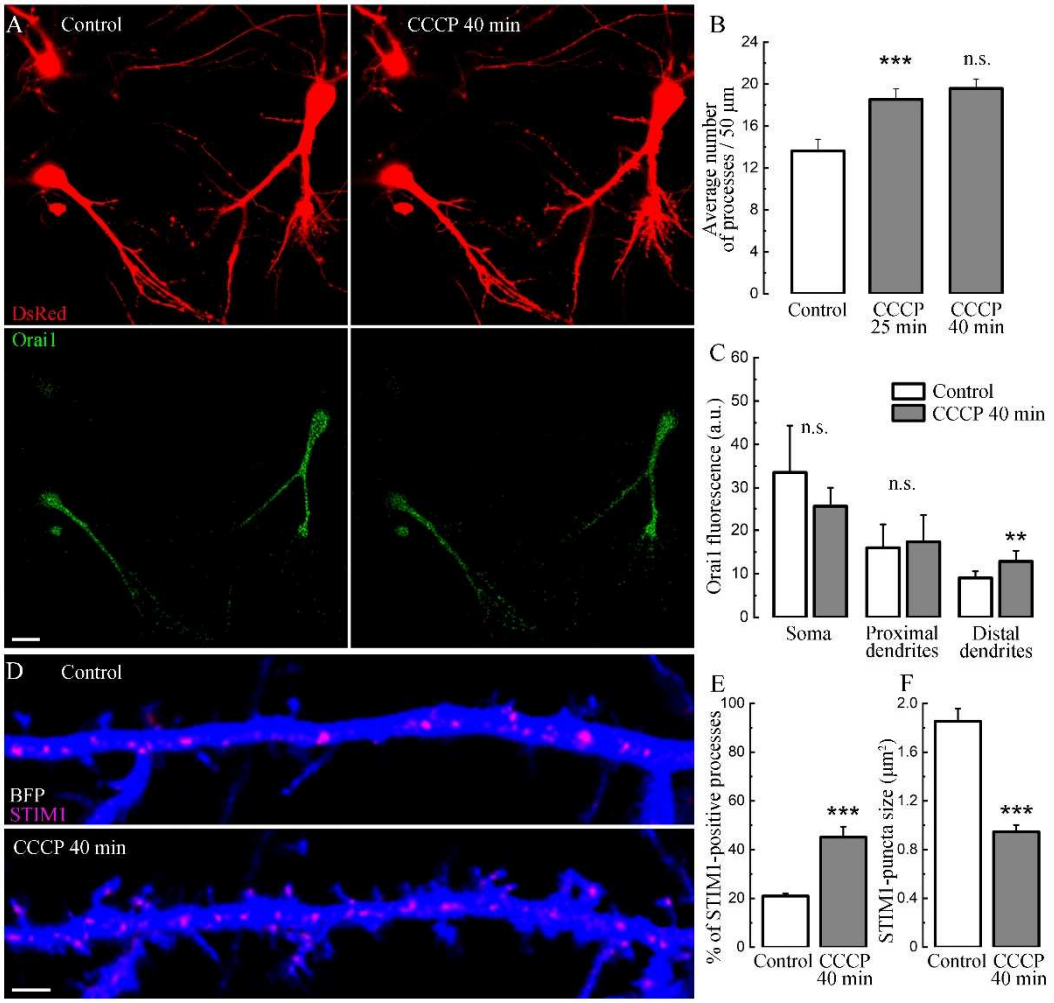

Figure 3. Effect of CCCP on Orai1/STIM1 fluorescence. A. Cells in control medium and after 40 min with CCCP which are transfected morphological marker DsRed (two upper panels). The same cells were transfected with normal Orai1 (green, bottom two panels, in control medium and after 40 min of CCCP). Scale 10 µm. **B.** Number of newly processes in control medium and after 25 and 40 min with CCCP treatment, n = 15 cells, three cultures, ANOVA, Bonferroni Post-hoc. **C.** Orai1 fluorescence level in control and after 40 minutes of CCCP treatment in soma, proximal and distal dendrites, n as in B, t-tests. **D.** Dendrite section from neuron transfected with BFP and STIM1 in control and after 40 minutes incubation with CCCP. STIM1-puncta translocated into existing and newly formed processes. **E.** Percentage of STIM-1 positive processes in control and after CCCP (20.97 ± 1.06 / 45.14 ± 4.28 ***, $p < 0.001$, t-test). **F.** The average STIM1-puncta in control and after 40 minutes of CCCP. For **E&F**: n = 18 cells, t-test, three cell cultures DIV 18-21.

In addition to a sharp increase in $[Ca^{2+}]i$, long-term treatment with CCCP also led to an increase in mitochondrial calcium ($[Ca^{2+}]m$). We detected an initial weak followed by a sharp increase in the fluorescence of the mitochondrial calcium sensor mtRCaMP against the background of a gradual increase in $[Ca^{2+}]i$ (Figure 4, A). A significant increase in $[Ca^{2+}]m$ was recorded at 30 minutes of treatment with the drug (Figure 4, B). The time lapse recording of new protrusion outgrowth and $[Ca^{2+}]m$ rise following CCCP is shown on supplementary video S2. It is interesting to note that occasionally we observed a staged "ignition" of mitochondria along the dendrite. An example of such a chain-like increase is shown in supplementary video S3. Another effect of CCCP on mitochondria was a significant decrease in the length of mitochondrial clusters, detected using the morphological mitochondrial sensor, mtDsRed (Figure 4, C). After 1 hour with CCCP, mitochondrial clusters significantly decreased in length, acquiring a ring/round shape (Figure 4, C, D).

Preprints (www.preprints.org) | NOT PEER-REVIEWED | Posted: 4 August 2023 doi:10.20944/preprints202308.0380.v1

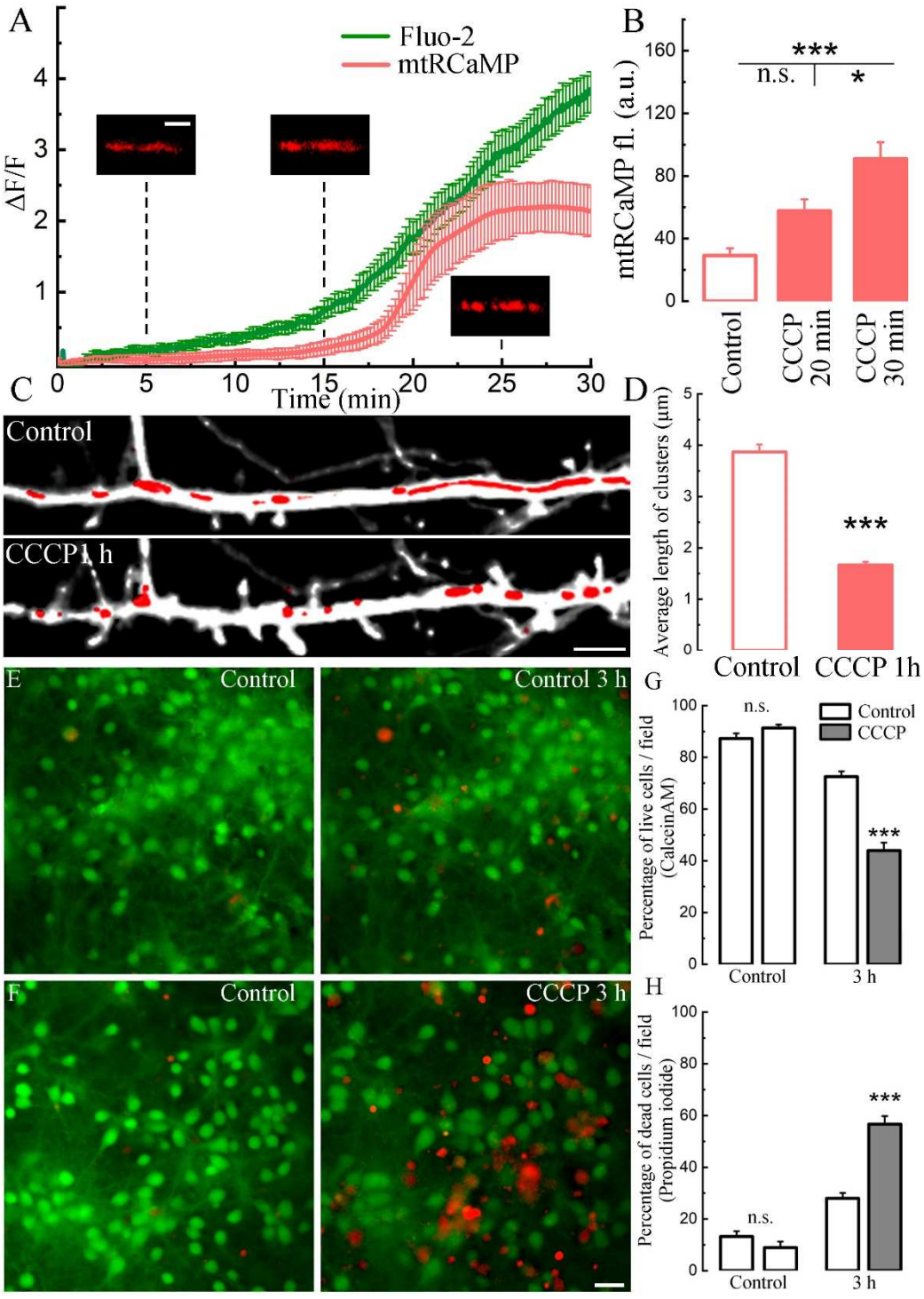

Figure 4. Effect of CCCP on mitochondria and cell survival. A. Mean Fluo-2 (green trace, from Figure 1, B, same experiment) conjugate with mtRCaMP fluorescence from 8 cell (bars indicate SEM). Small panels scale 2 μm. **B.** Averaged mtRCaMP fluorescence in control conditions, 20 min and 30 min after treatment with CCCP. Control (normal medium): 29.15 ± 4.62, 20 min CCCP: 57.67 ± 7,47, 30 min CCCP: 90,88 ± 10,7 a.u.; F = 14.95; * $p < 0.05$, *** $p < 0.001$, ANOVA, Bonferroni Post-hoc, n = 15, three cell cultures DIV 10-14. **C.** Dendrite segment in control and under CCCP conditions for 1 hour. Morphological sensor eBFP (monochrome), mitochondrial morphological sensor mtDsRed (red). Scale 5 μm. **D.** Average length of mitochondrial clusters (μm) in control and after 1 hour of treatment with CCCP (3.87 ± 0.15 / 1.67 ± 0.06, *** $p < 0.001$), n = 15 cells, t-test, three cell cultures DIV 10-14. **E&F.** Cells loaded with calcein AM (green), a marker of viable cells and propidium iodide, a marker of dead cells (red) in control and after 3 hours with CCCP. **C.** Percent of living cells (with calcein-AM) in

Preprints (www.preprints.org) | NOT PEER-REVIEWED | Posted: 4 August 2023 doi:10.20944/preprints202308.0380.v1

control medium and with CCCP before and after 3 hours of imaging at room temperature (RT). Control / Control: n.s.; Control 3 h / CCCP 3 h: ***, $p < 0.001$. **D.** Percent of dead cells (with propidium iodide) in control medium and with CCCP before and after 3 hours of imaging RT. Control / Control: n.s.; Control 3 h / CCCP 3 h: ***, $p < 0.001$. **For E&G:** values are mean ± SEM, n (control) = 52, n (CCCP) = 60 fields, t-tests.

We also tested whether apoptotic effects were associated with long-term imaging by keeping control cells and cells treated with 10 μM CCCP at room temperature for 2 and 5 hours (Supplementary Figure 3, A&B). The calculation of live cells in control and with CCCP after 5 hours showed a significant decrease in the number of healthy cells on coverslips with CCCP (Supplementary Figure 3, C&D). The number of dead cells was significantly higher with CCCP after 2 hours and especially 5 hours of exposure (ibid). The described visualization method gives a good idea of the advanced stages of cell death, when their structural destruction is visually obvious. Therefore, the effect is best manifested only after five hours of incubation. A more sensitive method for assessing acute cell death, the dead/live analysis [18,19], makes it possible to observe signs of death much earlier. To do this, we loaded cells with Calcein AM, a cell morphological marker, and performed the assay in the presence of propidium iodide (Figure 4, E&F). A feature of propidium iodide is that it does not cross the intact cell membrane. However, after perforation of the membrane, the substance enters the nucleus and intercalates between DNA strands. This method made it possible to determine which cells were alive before, and died after exposure to CCCP. Percentage of living cells after 3 hours of exposure to CCCP decreased from 91% to 44%, while in the control medium the decrease was only from 87% to 72%. The percentage of dead cells at the start of the experiment in the control media was 13 and 9%, after 3 hours 28% for the control and 56% for the CCCP: control / control n.s., $p > 0.05$; after 3 hours: control / CCCP 3 h ***, $p < 0.001$ (Figure 4, G&H).

3. Discussion

The carbonyl cyanide proton ionophore CCCP have been studied in various cell types. The main target for CCCP is the mitochondria: CCCP is used to study mitochondrial morphology, membrane potential, mitochondrial calcium, and ATP production. The CCCP-effect on $[Ca^{2+}]i$ has been shown in several studies of neurons [20–22] and non-neuronal cells [23–26], however no effect of CCCP on neuronal morphology has been demonstrated. Here, we show the effect of sustained CCCP-induced $[Ca^{2+}]i$ -rise on dendritic morphology. In our recent article, we demonstrated that application of 10 μM CCCP for 10 minutes completely abolished global calcium events in cultured hippocampal neurons [14]. However, longer-term treatment with CCCP lead to abnormally high $[Ca^{2+}]i$ levels, which are accompanied by the appearance of new filopodia and growth of existing processes. This increase of $[Ca^{2+}]i$ is probably due to the influx of extracellular calcium into the cell, since the effect does not appear in the nominal absence of calcium in the imaging medium. The CCCP effect of calcium influx was not blocked by APV (selective NMDA receptor antagonist) + TTX (a sodium channels blocker) + DNQX (a competitive antagonist of AMPA receptors) with the help of which excitatory synaptic potentials and backpropagation action potentials, and activity-induced calcium transients were blocked. Besides, the application of nifedipine (L-type VGCC blocker [27]) and ω-conotoxin (N-type VGCC blocker [28] did not block these CCCP-effects. Only slight $[Ca^{2+}]i$ decreased by thapsigargin, SERCA pump inhibitor against the background of CCCP (Figure 2, C). However, high concentrations (50 μM) of 2-APB, a blocker of Orai1,2-mediated Ca^{2+} -entry [29] prevented the increase of cytosolic calcium, as well as the growth of spines/filopodia.

We measured the number of new processes with CCCP in categories; filopodia/thin, mushroom and stubby spines. The majority of new processes are filopodia and few stubby and mushroom spines (Supplementary Figure 2, C). However, already existing spines/filopodia may undergo morphological changes with CCCP, as a result of which their assignment to one or another group changes (Figure 1, B; Supplementary Figure 2, A&B).

The present results demonstrate that exposure to CCCP for 20-30 minutes can cause a dramatic effect on formation of dendritic filopodia, via a sustained rise in $[Ca^{2+}]i$. These results do not allow us

 doi:10.20944/preprints202308.0380.v1

to speculate at the present time if these processes are to be converted to functional dendritic spines, since further treatment with CCCP leads to apoptotic swelling and cell death, as shown in the panels of Figure 2, E, F and Figure 4, F. In earlier studies we [13] and others [30] suggested that in normal conditions filopodia are produced at growth cones, as a means to attract the parent neuron to nearby excitatory afferents, and once they attach to these afferents they convert to functional synapses. Further experiments are needed to explore new grown / overgrown filopodia / spines.

It is noteworthy that under CCCP, the $[Ca^{2+}]m$ increased at different rates during the experiment (Figure 4, A). In addition, this calcium increase was not observed simultaneously in all mitochondrial clusters, but appeared sequentially (supplementary video S3). Concerning the effect of CCCP on the length of mitochondrial clusters, our results are consistent with previously demonstrated studies [31] showed that the morphological transition from "filamentous" to shortened, rounded structures depends on $[Ca^{2+}]i$, and the use of a protonophore-uncoupler leads to mitochondrial fission and/or sharp shortening/rounding or fragmentation of mitochondria, as well as to the formation of circular mitochondria. CCCP makes the mitochondrial inner membrane permeable to protons, with the result that electron transfer through the electron transport chain is no longer associated with ATP formation due to the loss of the electrochemical gradient [32]. Direct interference of CCCP with mitochondrial functions induces apoptosis by ultrastructural disruption of mitochondria and dissipation of mitochondrial membrane potential, triggering different stress pathways. CCCP-induced depletion of the antioxidant glutathione in mitochondria leads to increased oxygen species production with subsequent cell death. However, for a limited time, cultured cells are able to adapt by developing protective mechanisms against CCCP-induced apoptosis [33]. This study also confirms earlier reports on the involvement of Orai1 and STIM1 in the mechanisms of apoptosis [34] and CCCP effects, and also sheds light on concomitant processes CCCP-induces apoptosis, occurring in neurons that previously went unnoticed. Since oxidative stress and mitochondrial dysfunction are aggravating factors in many neurodegenerative diseases, more investigation is needed to test the role of $[Ca^{2+}]m$ in cell death.

The contrast between the early filopodial growth and the later apoptotic process is interesting indeed. After all, other plasticity processes associated with spine formation are not followed by cell death. To examine more closely the transition from spine/filopodia formation to apoptosis, we employed continuous recording of synaptic currents in cells exposed to CCCP. While the analysis of this study is still in progress, and will hopefully be presented in a follow-up study, suffice to say that spontaneous miniature synaptic currents increase in frequency over time after initial exposure to the drug, in association with the growth process, and not with the apoptotic process, but a clearer picture of this change awaits further analysis.

Finally, with regard to the formation of new filopodia or spine-like processes, we have shown in previous publications [13,17] that this growth occurs with the participation of the STIM-Orai system, due to which peculiar “hot spots” are created on the surface of dendrites. In essence, they are localized zones of calcium seepage into the cytosol through the STIM-Orai channels, which cause the growth of new filopodia. In the cases described above, CCCP seems to act only as a trigger for the massive growth, which in itself does not depend on the presence of the drug.

4. Materials and Methods

Cultures: Animal handling was done in accordance with the guidelines published by the Institutional Animal Care and Use Committee of the Weizmann Institute and with the Israeli National guidelines on animal care. Cultures were prepared as detailed elsewhere [35,36]. Briefly, E17 rat embryos were removed from pregnant decapitated mother's womb under sterile conditions, decapitated and their brains removed, the hippocampi were dissected free and placed in a chilled (4°C), oxygenated Leibovitz L15 medium (Gibco) enriched with 0.6% glucose and gentamicin (Sigma, 20μg/ml). Tissue was mechanically dissociated with a fire-polished pasteur pipette and passed to the plating medium consisting of 5% heat inactivated horse serum (HS), 5% fetal calf serum (FCS), prepared in MEM-Earl salts (Biological Industries), enriched with 0.6% glucose, Gentamicin, and 2 mm glutamax. About 10^5 cells in 1 ml medium were plated in each well of a 24 well plate onto

polylysine-coated 13 mm circular glass coverslips. Cells were left to grow in the incubator at 37°C, 5% CO2.

Plasmids: Neurons were transfected with Orai1-GFP, dominant negative Orai1 [37], a gift from Dr. E. Reuveny, the Weizmann Institute), STIM1-mCherry, DsRed or mtRCaMP, eBFP or eGFP (to image cell morphology), using lipofectamine2000 at 1 µl per well with 50 µl per well Opti-MEM (Invitrogen), at 6-7 days in-vitro (DIV) and were used for imaging at 10-21 DIV, depending on experiment. The transfection methodology was adopted from standard protocols [13].

Imaging: Fluo-2 AM (2 µM, Invitrogen) or Calcium Orange AM was incubated for 1 hour at room temperature to image variations in $[Ca^{2+}]i$. Cultures were then placed in the 3 mL perfusion chamber, on the stage of an upright Zeiss 880 confocal microscope using a 40× water immersion objective (1.0 NA), and imaged at a rate of frame / 3, 5 or 10 s. No photobleaching was detected under these conditions. Standard recording medium contained (in mM); NaCl 129, KCl 4, MgCl2 1, CaCl2 2, glucose 10, HEPES 10, pH was adjusted to 7.4 with NaOH, and osmolality to 320 mOsm with sucrose. All measurements were conducted with identical laser parameters for all groups (e.g., intensity, optical section, duration of exposure and spatial resolution) at room temperature.

Drugs: Preincubation with blockers tetrodotoxin (TTX, 1 µM) + 2-amino-5-phosphonovaleric acid, (APV) 30 µM) and 6,7-dinitroquinoxaline-2,3-dione (DNQX, 10 µM), thapsigargin 1 µM, nifedipine (1 µM) + ω-conotoxin (50 nM), 2-aminoethoxydiphenyl borate, (2-APB, 50 µM), all from Sigma-Aldrich, were made 10 minutes before the start of the recordings with CCCP (10 µM). For the wash experiment, drug was considered to be completely washed out the chamber after replacing the entire volume of the chamber three times.

Assessing acute cell death, the dead/live assay: Cells are initially loaded in 3ml standard recording medium with pre-incubation 2 µM calcein-AM in the presence of 2.5 µM propidium iodid (PI) at room temperature and imaged on a stage of a Zeiss LSM 880 confocal microscope using a 20× water immersion objective (1.0 NA). Time lapse imaging of cultures is performed at room temperature for 180 min at 1 min intervals. Two-channel images [Calcein AM / PI] are acquired, where green (488 nm) and red (545 nm) fluorescent cells represent live and dead cells, respectively. Percentage of live and dead cells is calculated as: live cells (cells stained green) or dead/dying cells (cells stained red) multiplied by 100% and divided by the total number of cells (green and red) in the field 200 x 200 micron at t = 0. Cells that either lose their color (Calcein-AM leaked out) or gain red staining (PI entering the cell) were not regarded as live (Supplementary Figure 3, A&B). Standard imaging software (Image J) is used to count the number of live cells for each image.

Fluorescence and statistical analysis: High-resolution fluorescent images were analyzed using Image-J (NIH, Bethesda, MD, USA) and MATLAB (R2010b, MathWorks, Inc., Natick, MA, USA)-based programs. Statistical comparisons were made with post hoc tests using ANOVA and t-tests, as the case may be, using MATLAB, KaleidaGraph (Synergy, Inc., Reading, PA, USA), and Origin (Electronic Arts, Inc., San Mateo, CA, USA) software. Statistically significant differences were considered at $p < 0.05$. Dendritic spines/filopodia were identified in the eBFP or DsRed-transfected neurons, and analyzed independently of the measurements of calcium.

Supplementary Materials: The following supporting information can be downloaded at the website of this paper posted on Preprints.org. Supplementary video S1. Effect of CCCP on the morphology of hippocampal neuron. Continuous time lapse imaging of morphological changes in eBFP-transfected neuron in the presence of CCCP was performed during about 31 min (pre-incubation with CCCP 10 minutes, not shown, to avoid bleaching) at the rate of 0.33 frame/s. In the video file, 1 min = 1 s. Frame size is about 211 x 74 µm. Note new protrusion appearance at 10th min video (20th min with CCCP) and first signs of dendrite blabbing at about 20th min (30th min with CCCP). Supplementary video S2. Effect of CCCP on new protrusion outgrowth and mitochondrial calcium rise in a dendritic segment of hippocampal neuron. Neuron was co-transfected with eBFP (morphology, cyan) and mtRCaMP (mitochondrial calcium, red). The video represents recording during about 37 min. In the video file, 3 min = 1 s. The frame size is about 93 x 9.5 µm. Note new protrusion appearance and influx of calcium into mitochondria at about 18th min of recording. Supplementary video S3.

Sequential calcium influx into mitochondria, stretched along the dendrite of hippocampal neuron. The cell was transfected with mitochondrial calcium-sensitive protein mtRCaMP. Cytosolic calcium indicator Fluo-2AM was loaded prior to imaging. Video recording was performed during 30 min. In the video file, 1 min = 1 s. The frame size is about 145 x 19.5 μm. Top frame, Fluo-2 fluorescence, green. Bottom frame, mtRCaMP fluorescence, red. Note the beginning of cytosolic calcium rise at about 12th min and the initiation of calcium influx into mitochondria starting from the left to the right of the frame at about 19th min.

Author Contributions: Conceptualization, EK and MS.; methodology, EK and LK.; software, EK and LK.; formal analysis, LK.; investigation, LK.; resources, MS.; data curation, LK.; writing—original draft preparation, LK, EK and MS.; visualization, LK.; supervision, MS.; project administration, MS. All authors have read and agreed to the published version of the manuscript.

Funding: This research received local Institutional funding.

Conflicts of Interest: The authors declare no conflict of interest.

References

1. Kushnireva, L.; Korkotian, E.; Segal, M. Calcium Sensors STIM1 and STIM2 Regulate Different Calcium Functions in Cultured Hippocampal Neurons. *Front Synaptic Neurosci.* **2021**, *12*, 573714. doi: 10.3389/fnsyn.2020.573714.
2. Bogeski, I.; Kilch, T.; Niemeyer, B.A. ROS and SOCE: recent advances and controversies in the regulation of STIM and Orai. *J Physiol.* **2012**, *590*, 4193-200. doi: 10.1113/jphysiol.2012.230565.
3. Feske, S.; Gwack, Y.; Prakriya, M.; Srikanth, S.; Puppel, S.H.; Tanasa, B.; Hogan, P.G.; Lewis, R.S.; Daly, M.; Rao A. A mutation in Orai1 causes immune deficiency by abrogating CRAC channel function. *Nature* **2006**, *441(7090)*, 179-85. doi: 10.1038/nature04702.
4. Skibinska-Kijek, A.; Wisniewska, M.B.; Gruszczynska-Biegala, J.; Methner, A.; Kuznicki, J. Immunolocalization of STIM1 in the mouse brain. *Acta Neurobiol Exp (Wars)* **2009**, *69(4)*, 413-28.
5. Klejman, M.E.; Gruszczynska-Biegala, J.; Skibinska-Kijek, A.; Wisniewska, M.B.; Misztal, K.; Blazejczyk, M.; Bojarski, L.; Kuznicki, J. Expression of STIM1 in brain and puncta-like co-localization of STIM1 and ORAI1 upon depletion of $Ca^{(2+)}$ store in neurons. *Neurochem Int* **2009**, *54(1)*, 49-55. doi: 10.1016/j.neuint.2008.10.005.
6. Mitchell, C.B.; Gasperini, R.J.; Small, D.H.; Foa, L. STIM1 is necessary for store-operated calcium entry in turning growth cones.J *Neurochem.* **2012**, *122(6)*, 1155-66. doi: 10.1111/j.1471-4159.2012.07840.x.
7. Pavez, M.; Thompson, A.C.; Arnott, J.H.; Mitchell, C.B.; D'Atri, I.; Don E.K.; Chilton, J.K.; Scott, E.K.; Lin, J.Y.; Young, K.M.; Gasperini, R.J.; Foa, L. STIM1 Is Required for Remodeling of the Endoplasmic Reticulum and Microtubule Cytoskeleton in Steering Growth Cones. *Journal of Neuroscience* **2019**, *39(26)*, 5095-5114. doi: 10.1523 /JNEUROSCI.2496-18.2019.
8. Park, C.Y.; Shcheglovitov, A.; Dolmetsch, R. The CRAC channel activator STIM1 binds and inhibits L-type voltage-gated calcium channels. *Science*, **2010**, *330(6000)*, 101-5. doi: 10.1126/science.1191027.
9. Steinbeck, J.A.; Henke, N.; Opatz, J.; Gruszczynska-Biegala, J.; Schneider, L.; Theiss, S.; Hamacher, N.; Steinfarz, B.; Golz, S.; Brüstle, O.; Kuznicki, J.; Methner, A. Store-operated calcium entry modulates neuronal network activity in a model of chronic epilepsy. *Exp Neurol.* **2011**, *232(2)*, 185-94. doi: 10.1016/j.expneurol.2011.08.022.
10. Zhang, M.; Song, J.N.; Wu, Y.; Zhao, Y.L.; Pang, H.G.; Fu, Z.F.; Zhang, B.F.; Ma, X.D. Suppression of STIM1 in the early stage after global ischemia attenuates the injury of delayed neuronal death by inhibiting store-operated calcium entry-induced apoptosis in rats. *Neuroreport* **2014**, *25(7)*, 507-13. doi: 10.1097/WNR.0000000000000127.
11. Henke, N.; Albrecht, P.; Bouchachia, I.; Ryazantseva, M.; Knoll, K.; Lewerenz, J.; Kaznacheyeva, E.; Maher, P.; Methner, A. The plasma membrane channel ORAI1 mediates detrimental calcium influx caused by endogenous oxidative stress. *Cell Death Dis.* **2013**, *24*, 4:e470. doi: 10.1038/cddis.2012.216.
12. Keil, J.M.; Shen, Z.; Briggs, S.P.; Patrick, G.N. Regulation of STIM1 and SOCE by the ubiquitin-proteasome system (UPS). *PLoS One* **2010**, *5(10)*, e13465. doi: 10.1371/journal.pone.0013465.
13. Korkotian, E.; Oni-Biton, E.; Segal, M. The role of the store-operated calcium entry channel Orai1 in cultured rat hippocampal synapse formation and plasticity. *J Physiol.* **2017**, *595(1)*, 125-140. doi: 10.1113/JP272645.
14. Kushnireva, L.; Basnayake, K.; Holcman, D.; Segal, M., Korkotian, E. Dynamic Regulation of Mitochondrial $[Ca^{2+}]$ in Hippocampal Neurons. *Int. J. Mol. Sci.* **2022**, *23(20)*, 1232123. doi: 10.3390/ijms232012321 12321.

15. Poncer, J.C.; McKinney, R.A.; Gähwiler, B.H.; Thompson, S.M. Either N- or P-type calcium channels mediate GABA release at distinct hippocampal inhibitory synapses. *Neuron* **1997**, *18(3)*, 463-72. doi: 10.1016/s0896-6273(00)81246-5.
16. Peckys, D.B.; Gaa, D.; Alansary, D.; Niemeyer, B.A.; Jonge, N. Supra-Molecular Assemblies of ORAI1 at Rest Precede Local Accumulation into Puncta after Activation. *Int J Mol Sci.* **2021**, *22(2)*, 799. doi: 10.3390/ijms22020799.
17. Korkotian, E.; Segal, M. Roles of calcium stores and store-operated channels in plasticity of dendritic spines, *Neuroscientist*, **2016**, *22(5),* 477-485. doi:10.1177/1073858415613277.
18. Slepian, M.J.; Massia, S.P.; Whitesell, L. Pre-conditioning of smooth muscle cells via induction of the heat shock response limits proliferation following mechanical injury. *Biochem Biophys Res Commun.* **1996,** *225(2),* 600-7. doi: 10.1006/bbrc.1996.1217.
19. Sadeh, N.; Oni-Biton, E.; Menahem Segal. Acute Live/Dead Assay for the Analysis of Toxic Effects of Drugs on Cultured Neurons. Bio-protocol 2016, 6(15), e1889. doi: 10.21769/BioProtoc.1889.
20. Shishkin, V.; Potapenko, E.; Kostyuk, E.; Girnyk, O.; Voitenko, N.; Kostyuk, P. Role of mitochondria in intracellular calcium signaling in primary and secondary sensory neurones of rats. *Cell Calcium* **2002**, *32(3)*, 121-30. doi: 10.1016/s0143-4160(02)00095-7.
21. de Oliveira, R.B.; Gravina, F.S.; Lim, R.; Brichta, A.M.; Callister, R.J.; van Helden, D.F. Heterogeneous responses to antioxidants in noradrenergic neurons of the Locus coeruleus indicate differing susceptibility to free radical content. *Oxid Med Cell Longev.* **2012**, *012*, 820285. doi: 10.1155/2012/820285.
22. Komori, Y.; Tanaka, M.; Kuba, M.; Ishii, M.; Abe, M.; Kitamura, N.; Verkhratsky, A.; Shibuya, I.; Dayanithi, G. $Ca^{(2+)}$ homeostasis; $Ca^{(2+)}$ signalling and somatodendritic vasopressin release in adult rat supraoptic nucleus neurones. *Cell Calcium* **2010**, *48(6),* 324-32. doi: 10.1016/j.ceca.2010.10.002.
23. Babcock, D.F.; Herrington, J.; Goodwin, P.C.; Park, Y.B.; Hille B. Mitochondrial participation in the intracellular Ca^{2+} network. J *Cell Biol.* **1997**, 136(4), 833-44. doi: 10.1083/jcb.136.4.833.
24. Ramachandran, R.P.; Spiegel, C.; Keren, Y.; Danieli, T.; Melamed-Book, N.; Pal, R.R.; Zlotkin-Rivkin, E.; Rosenshine, I.; Aroeti, B. Mitochondrial Targeting of the Enteropathogenic Escherichia coli Map Triggers Calcium Mobilization; ADAM10-MAP Kinase Signaling; and Host Cell Apoptosis. *mBio* **2020**, *11(5)*, e01397-20. doi: 10.1128/mBio.01397-20.
25. Herrington, J.; Park, Y.B.; Babcock, D.F.; Hille B. Dominant role of mitochondria in clearance of large Ca^{2+} loads from rat adrenal chromaffin cells. *Neuron* **1996**, *16(1)*, 219-28. doi: 10.1016/s0896-6273(00)80038-0.
26. Pereira, M.B.; Tisi, R.; Fietto, L.G.; Cardoso, A.S.; França, M.M.; Carvalho, F.M.; Trópia, M.J.; Martegani, E.; Castro, I.M.; Brandão, R.L. Carbonyl cyanide m-chlorophenylhydrazone induced calcium signaling and activation of plasma membrane H(+)-ATPase in the yeast Saccharomyces cerevisiae. *FEMS Yeast Res.* **2008**, *8(4)*, 622-30. doi: 10.1111/j.1567-1364.2008.00380.x
27. Plumbly W, Brandon N, Deeb TZ, Hall J, Harwood AJ. L-type voltage-gated calcium channel regulation of in vitro human cortical neuronal networks. *Sci Rep.* **2019,** *9(1)*, 13810. doi: 10.1038/s41598-019-50226-9.
28. Hannon, H.E.; Atchison, W.D. Omega-conotoxins as experimental tools and therapeutics in pain management. *Mar Drugs.* **2013**, *11(3)*, 680-99. doi: 10.3390/md11030680.
29. Putney, J.W. Pharmacology of store-operated calcium channels. *Mol Interv.* **2010**, *10(4)*, 209-18. doi: 10.1124/mi.10.4.4.
30. Abe Kentaro Chisaka, Osamu, van Roy Frans & Takeichi Masatoshi. Stability of dendritic spines and synaptic contacts is controlled by αN-Catenin. *Nature Neuroscience*, **2004,** 7(4).
31. Brustovetsky, T.; Li, V.; Brustovetsky, N. Stimulation of glutamate receptors in cultured hippocampal neurons causes Ca^{2+}-dependent mitochondrial contraction. *Cell Calcium* **2009**, *46(1),* 18-29. doi: 10.1016/j.ceca.2009.03.017.
32. de Graaf, A.O; van den Heuvel, L.P; Dijkman, H.B; de Abreu, R.A; Birkenkamp, K.U; de Witte, T; van der Reijden, B.A; Smeitink, J.A; Jansen, J.H. Bcl-2 prevents loss of mitochondria in CCCP-induced apoptosis. *Exp Cell Res.* **2004**, *299(2),* 533-40. doi: 10.1016/j.yexcr.2004.06.024.
33. Kane, M.S; Paris, A; Codron, P; Cassereau, J; Procaccio, V; Lenaers, G; Reynier, P; Chevrollier, A. Current mechanistic insights into the CCCP-induced cell survival response. *Biochem Pharmacol.* **2018**, *148*, 100-110. doi: 10.1016/j.bcp.2017.12.018.
34. Henke, N.; Albrecht, P.; Pfeiffer, A.; Toutzaris, D.; Zanger, K.; Methner, A. Stromal interaction molecule 1 (STIM1) is involved in the regulation of mitochondrial shape and bioenergetics and plays a role in oxidative stress. *J Biol Chem.* **2012**, *287(50),* 42042-52. doi: 10.1074/jbc.M112.417212.
35. Vlachos, A.; Korkotian, E.; Schonfeld, E.; Copanaki, E.; Deller, T. and Segal, M. Synaptopodin regulates plasticity of dendritic spines in hippocampal neurons. *J. Neurosci.* **2009**, *29*, 1017-1033. doi: 10.1523/JNEUROSCI.5528-08.2009.
36. Korkotian, E.; Meshcheriakova, A.; Segal M. Presenilin 1 Regulates $[Ca^{2+}]i$ and Mitochondria/ER Interaction in Cultured Rat Hippocampal Neurons. *Oxid Med Cell Longev.* **2019** *2019*, 7284967. doi: 10.1155/2019/7284967.

37. Zhang, S.L.; Yeromin, A.V.; Hu, J.; Amcheslavsky, A.; Zheng, H.; Cahalan, M.D. Mutations in Orai1 transmembrane segment 1 cause STIM1-independent activation of Orai1 channels at glycine 98 and channel closure at arginine 91. *Proc Natl Acad Sci U S A.* **2011**, *108(43)*, 17838-43. doi: 10.1073/pnas.1114821108.